The Influence of the Alcohol Concentration on the Structural Ordering of Mesoporous Silica: Cosurfactant versus Cosolvent

Shiquan Liu,[†] Pegie Cool,*,[‡] Olivier Collart,[‡] Pascal Van Der Voort,[‡] Etienne F. Vansant,[‡] Oleg I. Lebedev,[§] Gustaaf Van Tendeloo,[§] and Minhua Jiang[⊥]

Laboratory of Adsorption and Catalysis, University of Antwerpen (UIA), Universiteitsplein 1, 2610 Wilrijk, Belgium, School of Materials Science and Engineering, Jinan University, 250022 Jinan, Shandong, China, School of Materials Science and Engineering, Shandong University, 250100 Jinan, Shandong, China, and EMAT, University of Antwerpen (RUCA), Groenenborgenlaan 171, 2020 Antwerpen, Belgium

Received: February 18, 2003; In Final Form: July 9, 2003

Increasing the ethanol concentration in the tetraethoxysilane (TEOS)−hexadecyltrimethylammmonium bromide (C_{16}TMABr)−ammonia−water system at room temperature permits one to obtain a succession of different mesophases in the order MCM-41 → MCM-48 → lamellar phase → radial hexagonally ordered phase. First, the original hexagonal (MCM-41) phase is replaced by a cubic phase (MCM-48) and later, upon ethanol addition, by a lamellar phase. Such phase succession is the result of the cosurfactant behavior of the ethanol. At lower alcohol concentration, scanning electron microscopy (SEM) shows only undefined or barely spherical structures, indicating that the ethanol has only a limited effect on the external morphology. When the alcohol concentration is further increased, it will mainly act as a cosolvent producing spherical particles. A TEM study reveals the radial arrangement of the pores within the spherical particles. A hexagonal closed pore packing can be considered on a local scale around the center of the spherical particle. This hexagonal pore arrangement is the result of a combination of a very slow equilibrium toward the hydrolysis of the TEOS, its good homogenization in the synthesis solution due to the solvating effect of the alcohol, and the interference of the alcohol on the cooperative process of the micelle formation. To complete the study, parallels have been drawn with other alcohols such as methanol and propanol.

Introduction

During the past decade, mesoporous materials of the M41S family have attracted worldwide attention.[1−6] These materials have unique properties, such as a high specific surface area and pore volume, tuneable pore size, and a narrow pore size distribution.

In this M41S family, three main mesophases have been described. The most well-known structure is the hexagonal MCM-41.[7] The other two phases are the cubic MCM-48[8,9] and a lamellar phase, denoted as MCM-50. However the latter is an unstable phase that will collapse upon removal of the surfactant molecules. The ability to obtain a given structure is mainly dependent on the preferential organization of the organic phase. Huo et al.[10] dedicated those preferences for a particular phase to the *g*-packing parameter. They delimited the different *g*-packing values as being 0.5, 0.66, and 1 for the hexagonal, cubic, and lamellar phase, respectively.

The syntheses of those different phases have already been reported in many variants, in which the reactants, such as Si-source and type of surfactant, as well as the synthesis parameters, have been changed. Particular synthesis conditions permit the material even to favor a phase transition. This transformation is important in obtaining easily and quickly M41S phases that are otherwise relatively difficult to prepare. The best documented is the transition of a hexagonal phase to a cubic phase induced by a heating step. Besides temperature, also the importance of small amounts of ethanol, formed by the hydrolysis of the silicate source tetraethoxysilane (TEOS), is pointed out as the driving force for the transformations to occur by altering the surfactant packing parameter within the micellar surfactant templates.[11]

Most of the above-optimized syntheses are performed under hydrothermal conditions. A few researchers described the possibilities of obtaining different phases at room temperature. First, Ågren and co-workers[12] demonstrated the transition from an MCM-41 hexagonal structure into a lamellar phase by adding small quantities of large alcohols such as butanol and hexanol to the reaction mixture, resulting in the formation of a lamellar phase next to the hexagonal one. They attributed this phenomenon to the properties of some alcohol molecules to incorporate the micelles and adopt the role of cosurfactant. In this case, it is not a phase transition that is observed but the direct synthesis of a new phase.

Grün et al.[13] used the same mother solution (TEOS/NH_3/H_2O) as Ågren and co-workers but added large amounts of ethanol to the synthesis mixture. They did so to approach as much as possible the well-known Stöber synthesis.[14] This procedure is known to synthesize spherical silica particles under controlled conditions. Grün and co-workers indeed demonstrated the ability of controlling the morphology of these mesoporous particles, which they claimed to be MCM-41. Therefore they entrust the ethanol to a role of cosolvent without mentioning any cosurfactant effects. Pauwels et al.[15] performed a transmission electron

---

* To whom correspondence should be addressed. E-mail: pegie.cool@ua.ac.be.
[†] Jinan University.
[‡] University of Antwerpen (UIA).
[§] University of Antwerpen (RUCA).
[⊥] Shandong University.

10.1021/jp034410w CCC: $25.00

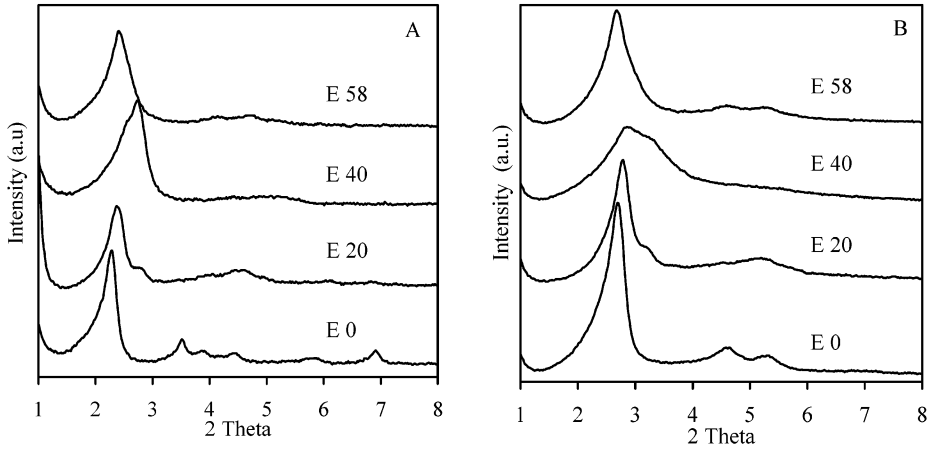

Figure 1. X-ray diffractograms of the different silica mesophases formed with increasing concentrations of ethanol: (A) precursor materials; (B) calcined materials.

microscopy (TEM) study on those spherical particles and could identify a radial arrangement of the pores.

The purpose of this paper is to investigate the influence on the structure of the mesoporous solids of the amount of short-chain alcohols [$C_nH_{2n+1}OH$, $n = 1, 2, 3$] in the TEOS−hexadecyltrimethylammmonium bromide (C_{16}TMABr)−ammonia−alcohol−water mixture at room temperature. For the first time, a systematic study of the influence of the alcohol addition on the morphology and structure of the mesoporous particle is performed. Up to high alcohol concentrations, the different phase transitions are studied. This is done using X-ray diffraction (XRD), N_2 sorption, scanning electron microscopy (SEM) and TEM analyses. The study mainly focuses on the influence of ethanol addition, though also the smaller methanol and the larger propanol are investigated.

Experimental Section

From a reference procedure for spherical MCM-41,[15] different amounts of ethanol, methanol, or propanol are added to obtain a gel with the following composition: 1 TEOS/0.3 C_{16}TMABr/11 NH_3/***x* alcohol**/144 H_2O. Accordingly, we denote the sample containing *x* mol (per mole of TEOS) of methanol, ethanol, or propanol as M*x*, E*x*, and P*x*, respectively.

To synthesize the material, C_{16}TMABr was first dissolved in the mixed solution of distilled water, aqueous ammonia, and alcohol by stirring for 15 min; then TEOS was added. The solution was further stirred for 2 h; the white precipitate was then collected by filtration and washed with distilled water. Dried samples were calcined at 550 °C with a heating rate of 1 °C/min and kept at this temperature for 6 h to remove the surfactant.

X-ray diffractograms were collected on a Philips PW1840 powder diffractometer (45 kV, 25 mA) using a Ni-filtered Cu Kα radiation at steps of 0.02° 2θ.

The N_2 adsorption isotherms were recorded on a Quantachrome Autosorb-1-MP automated gas adsorption system. The surface areas were calculated with the Brunauer−Emmett−Teller (BET) calculation method, using the adsorption data within the p/p_0 range from 0.05 to 0.35. For a rapid and easy pore diameter analysis the Barrett−Joyner−Halenda (BJH) method was preferred above the more accurate nonlinear density functional (NLDFT) theory. Although BJH is known to seriously underestimate the effective pore diameter, it is usable as a pure comparative method without considering the absolute values.

SEM images were recorded using a JEOL-JSM-6300 scanning electron microscope operating at an accelerating voltage of 20−30 kV. The samples were sputtered with a thin film of gold.

Transmission electron microscopy (TEM) investigations were made on crushed E0, E20, and E58 samples deposited on holey carbon grids using a JEOL 4000 EX microscope operating at 400 kV and Philips CM20 operated at 200 kV. In high-resolution electron micrscopy (HREM), a low-intensity electron beam and medium magnification were used to minimize damage of the structure. The HREM images were mostly taken at large underfocus conditions when tunnels are imaged as bright dots and matter as black.[16] Fourier transformation (FT) of the HREM images was performed using the NIH Image 1.60ppc software.

Results

A. The Influence of the Amount of Ethanol. Figure 1 represents the X-ray diffraction patterns for the different silica mesophases with an increasing addition of ethanol to the mother solution before (A) and after calcination (B). From the XRD of the calcined E0 (Figure 1B), it is clear that without any addition of ethanol, the synthesized material is a typical MCM-41. The good crystallinity is evidenced by a strong (100) diffraction peak at $2\theta = 2.69°$ and two other distinguishable peaks between 4° and 6°, attributed to the (200) and (210) reflections. Before calcination, additional peaks are detected because of the presence of surfactant. With the addition of 20 mol of ethanol in E20, the cubic MCM-48 phase is formed; this phase is identified by the two distinct (211) and (220) diffraction peaks at $2\theta = 2.79°$ and 3.03° and a broader reflection at 5.09° (Figure 1B). When the amount of ethanol is doubled in case of E40, part of the broad XRD signal disappears upon calcination (Figure 1B). This suggests that E40 consists of mixed mesophases, in which a lamellar mesophase is responsible for the pore collapse during the removal of the organic surfactant. The remaining signal points toward some ordered structure on a local scale; no clear structure identification is possible though. Further increasing the amount of ethanol to a mole ratio of 58 (sample E58) produces again an MCM-41-like diffraction pattern with a clear (100) reflection at 2.69° 2θ and two broader peaks in the region between 4° and 6° attributed to the (200) and (210) reflections (Figure 1B). Although a clear diffraction pattern, the peaks are broader compared to the E0 sample, indicating that this hexagonal-like E58 mesophase is less-ordered.

The isotherms of the different silica mesophases formed with increasing ethanol concentration (Figure 2) are of type IV in

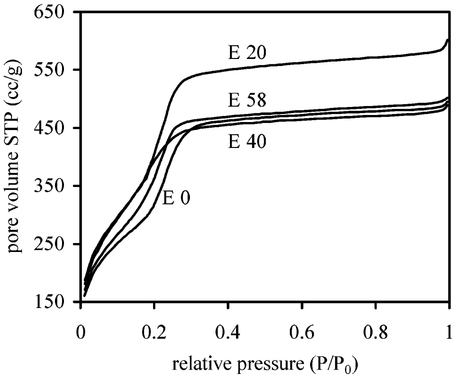

Figure 2. N_2 adsorption isotherms of the different silica mesophases formed with increasing concentrations of ethanol.

the IUPAC classification, showing a capillary condensation at a relative pressure p/p_0 between 0.2 and 0.3. The surface area, the pore volume, and the pore diameter of the E0 sample (MCM-41) are 1129 m^2/g, 0.707 mL/g, and 2.25 nm, respectively. The higher surface area of this MCM-41 compared to the ones prepared in hydrothermal conditions, as reported in the literature, is due to an artifact. With the decrease of the pore diameter, the capillary condensation step will undergo a left shift to lower relative pressures. This will influence the linearity of the multilayer deposition of the nitrogen, increasing its steepness. The surface areas given by the BET equation will therefore be overevaluated. With the change of mesophase from hexagonal (MCM-41) to cubic (MCM-48), the sample E20 (Figure 2) reveals a small decrease of the pore size to 2.20 nm but a significant increase for the surface area and pore volume, reaching now 1379 m^2/g and 0.819 mL/g, respectively. Upon further increase of the alcohol content to 40 mol ratio (E40, Figure 2), the isotherm represents a much less defined shape. Though the low-pressure region until $p/p_0 = 0.2$ is identical to that of sample E20 (cubic MCM-48), this is an indication that the remaining mesophase possesses a cubic symmetry. The isotherm data of the sample with the highest ethanol addition, E58, indicate an identical total pore volume for both E0 and E58 and a slightly smaller pore diameter for E58 (Figure 2). The surface area, pore volume, and pore diameter of E58 are, respectively, 1211 m^2/g, 0.707 mL/g, and 2.11 nm.

Scanning electron microscopy (SEM) shows the morphology of the different silica mesophase particles formed with increasing ethanol concentration (Figure 3). The MCM-41 particles (Figure 3A) have an irregular shape with a particle size of about 1 μm; no real spheres are observed. The same irregular morphology is found for the MCM-48 mesophase particles in E20 (Figure 3B). When the ethanol is further increased in sample E40, a clear change occurs: the mixed mesophase E40 mainly consists of spheres (Figure 3C), though there is still a large contribution of particles of an undefined shape. The dimension of the particles has decreased to 0.5−1 μm, compared to the previous ones. Finally, the E58 (Figure 3D) reveals small regular particles of perfectly spherical shape with average sizes of about 0.5 μm.

To identify further the order and the change in the pore arrangement of the different mesophases, a TEM study was performed. The HREM image of E0 taken along $[001]_H$ zone axis is shown in Figure 4. The image reveals a hexagonal arrangement of the pores in the MCM-41 phase; this is confirmed by the FT. The HREM image of E20 also shows a nicely ordered pore system (Figure 5). This structure however is cubic; the FT pattern (inset of Figure 5) reveals that the structure is imaged along the $[011]_C$ direction. It should be noted though that both samples exhibit a large quantity of disordered phases, which are responsible for the high amorphous background in the XRD patterns. It is also confirmed that there is no preference in the shape of the particles, in agreement with the SEM observations. The particles in the E58 sample on the other hand exhibit a pronounced spherical morphology (Figure

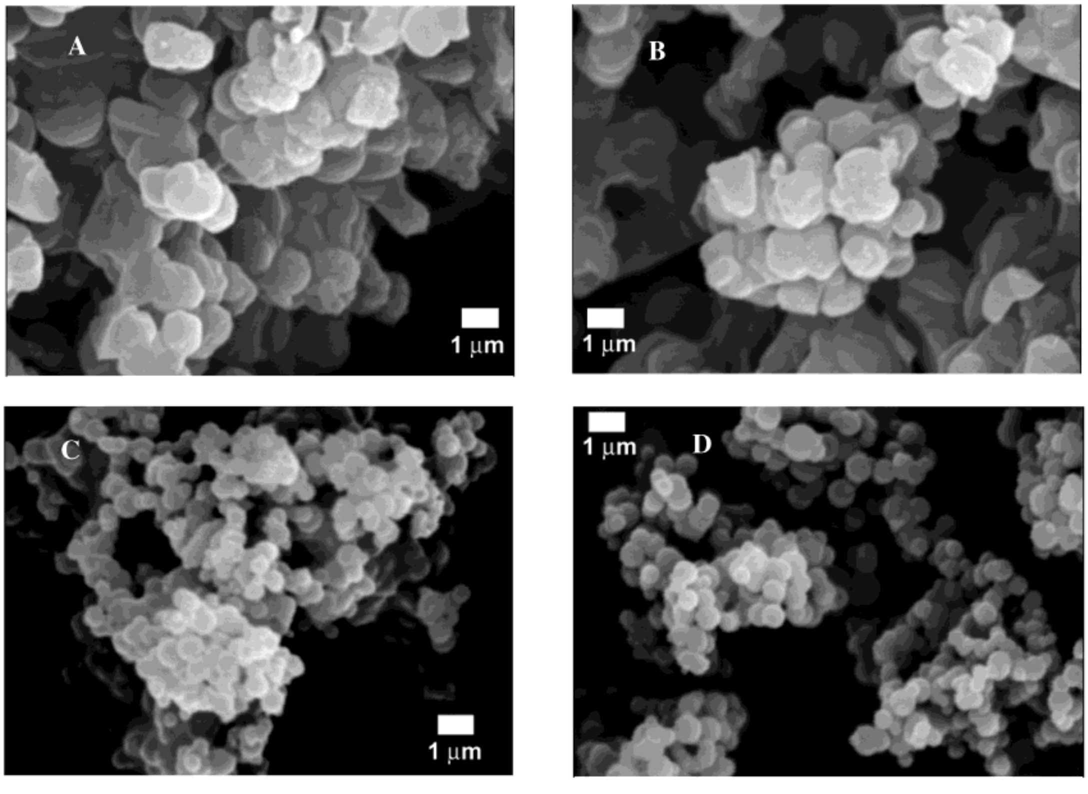

Figure 3. SEM images of the different silica mesophase particles formed with increasing concentrations of ethanol: (A) E0; (B) E20; (C) E40; (D) E58.

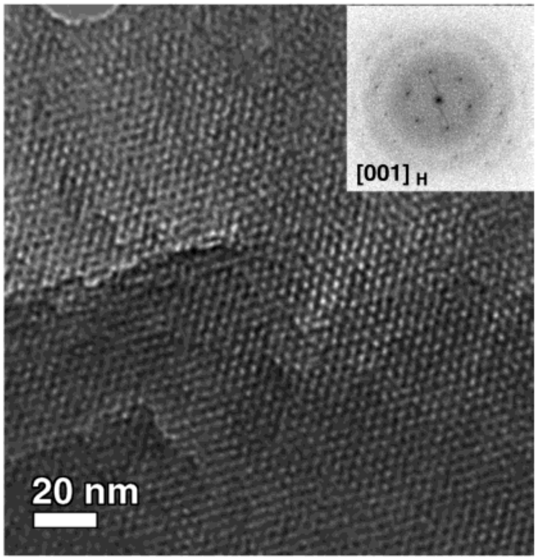

Figure 4. HREM image of MCM-41 hexagonal structure taken along the $[001]_H$ zone axis from E0 sample with Fourier transform insert.

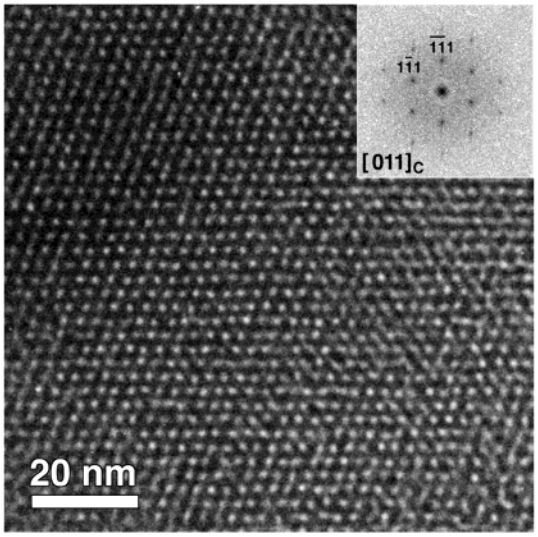

Figure 5. HREM image of MCM-48 cubic structure taken along the $[011]_C$ zone axis from E20 sample with indexed Fourier transform insert.

6). The center of the image shows a clear resolution, indicating a radial arrangement of the pores.[15] The image shows a hexagonal pore packing around the core of the particle. An additional proof of the hexagonal local structure is given by the FT pattern taken over the central part of the particle (inset Figure 6), where the hexagonal symmetry is reflected. The weakness of the spots in the FT pattern indicates that the hexagonal arrangement only occurs on a local scale and around the center part of the spherical particle. Deviations from the hexagonal symmetry are bound to occur because of the spherical shape of the particle.

B. The Influence of the Amount of Propanol and Methanol. To draw parallels with other alcohols, the influence of the addition of propanol or methanol to the reaction mixture of the mesophase formation was investigated.

Conclusions on the respective silica mesophase transitions that occur upon addition of propanol or methanol, similar to the ethanol addition, can be drawn from the X-ray diffraction patterns and N_2 adsorption data (Figures 7−10). Without the addition of any alcohol (P0 and M0), the same MCM-41 phase is obtained, as evidenced by the XRD patterns (Figures 7B and 9B). The addition of 8 mol of propanol or 65 mol of methanol to the reaction results in different mesophases. For methanol, this new phase is clearly MCM-48 (Figure 9B). A lower amount of methanol (58 mol) is not enough to favor the MCM-48 synthesis; in this case an MCM-41 mesophase is obtained with additional XRD peaks due to the surfactant before calcination (Figure 9A). In case of 8 mol of propanol, before calcination, an MCM-48 phase can be detected, although the diffraction peaks largely disappear after calcination, suggesting the existence of a mixed mesophase consisting of MCM-48 and a lamellar structure. The isotherms of the P8 and M65 mesophases show an enhanced adsorption in the low-pressure region up to $p/p_0 = 0.25$ (Figures 8 and 10). The surface areas and pore volumes are, respectively, 1270 m^2/g and 0.778 mL/g (P8) and 1239 m^2/g and 0.817 mL/g (M65). When the propanol concentration is further increased up to 14 mol, no diffraction peaks remain after calcination, indicating the significant loss in crystallinity. Also, the isotherm shows a strong decrease in the pore volume. These results suggest a collapse of the ordered pore structure and indicate that sample P14 is in fact a pure lamellar mesophase. For methanol, no lamellar phase transition occurs. Even a methanol concentration of 85 mol (M85) produces the MCM-48 mesophase. Upon further increasing the alcohol concentration to 30 mol (propanol) and 100 mol (methanol), the (100) diffraction between 2° and 3° 2θ is again observed in the XRD after calcination, indicating a hexagonal-like ordering. In case of methanol, two additional peaks occur in the region 5°−6° 2θ. The isotherm P30 again reveals a clear step in the adsorption (at $p/p_0 = 0.2-0.3$). The surface area and the pore volume are restored up to 1008 m^2/g and 0.778 mL/g. The M100 MCM-41-like material exhibits a surface area and pore volume of, respectively, 1298 m^2/g and 0.722 mL/g.

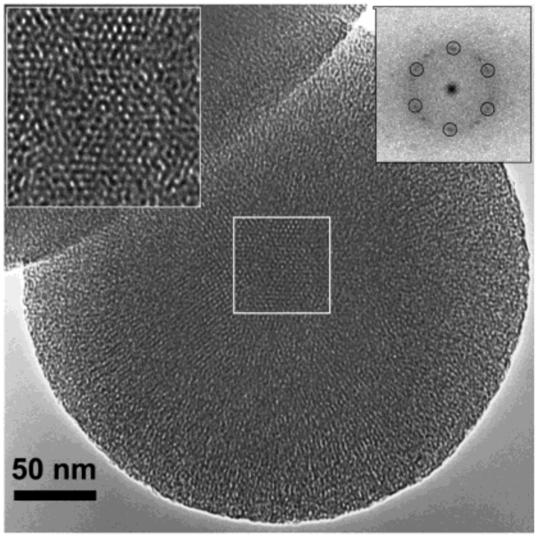

Figure 6. HREM image of a spherical particle with a well-resolved core, enlargement of the core (marked with a white square frame) given as insert in the left upper corner, and corresponding FT pattern (right upper corner) clearly showing the hexagonal symmetry. The 10−10 and 11−20 peaks of a hexagonal pattern (encircled) are clearly visible.

Discussion

Phase Transitions. In the TEOS−C_{16}TMABr−ammonia−water−ethanol system, a phase transition (MCM-41 to MCM-48) is identified by XRD and TEM for an increasing alcohol amount. The results suggest that increasing the alcohol amount changes the surfactant packing parameter, *g*. This surfactant packing parameter *g* directs the phase configuration in the

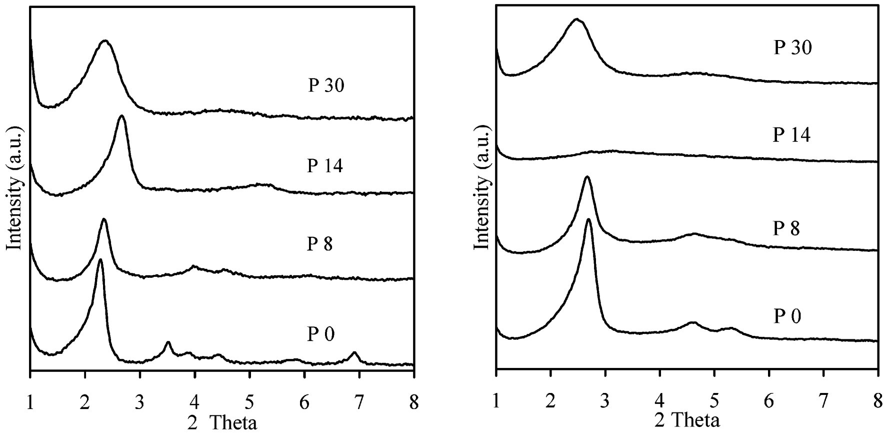

Figure 7. X-ray diffractograms of the different silica mesophases formed with increasing concentrations of propanol: (A) precursor materials; (B) calcined materials.

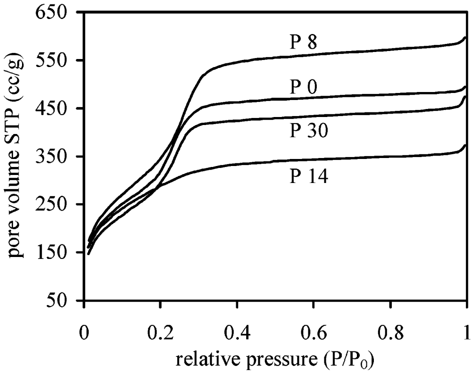

Figure 8. N_2 adsorption isotherms of the different silica mesophases formed with increasing concentations of propanol.

synthesis of mesoporous materials and is given by $g = V/(a_0 l)$, V being the total volume of the surfactant chain plus any cosolvent molecules between the chains, a_0 the effective headgroup area at the organic−inorganic interface, and l the surfactant chain length.[10] Small values of g stabilize more curved surfaces such as MCM-41 ($^1/_3 < g < {}^1/_2$), while larger values stabilize structures with less curvature such as MCM-48 ($^1/_2 < g < {}^2/_3$).

At the lower alcohol concentrations, driven by the hydrophobic forces, the alcohol molecules penetrate into the surfactant micelles. This results in an increase of the true volume of the surfactant and therefore in an increase of the g value causing high-to-low curvature phase transitions. Consequently, mesophases with less curvature are sequentially formed, going from hexagonal to cubic. This has been widely proven in many cases and is referred to as the cosurfactant effect of the alcohol.[10−12,17] As in previous studies, the syntheses are performed under hydrothermal conditions, and small amounts of ethanol released during the hydrolysis of TEOS are able to penetrate into the surfactant micelles, causing the transformation into a different phase. At room temperature however, the released ethanol from the hydrolysis reaction of TEOS will primarily reside at the outer shell of the surfactant micelles, explaining why in this study additional amounts of alcohol are needed to change the micellar volume and to induce the desired phase transition. The room temperature of the synthesis will also affect every further restructuring of the mesophase. Ågren[12] demonstrated with an in-situ XRD experiment that even at room temperature the mesophase formation is a relative fast process, inducing diffraction signals within a few minutes after the addition of the silica source. The low pH of the solution (pH 10.9 due to the use of ammonia as base) will favor the fast condensation of the hydrolyzed silica. In a classic hydrothermal synthesis, the high temperature, in combination with a high basicity (pH >12), creates the ideal conditions for redissolution[18] and reorganization of the amorphous phase into an organized mesophase. The unfavorable condition of this room-temperature synthesis for an eventual mesophase reorganization is the main reason for the presence of the amorphous phase revealed by the TEM analysis. The fast condensation and formation of the silica

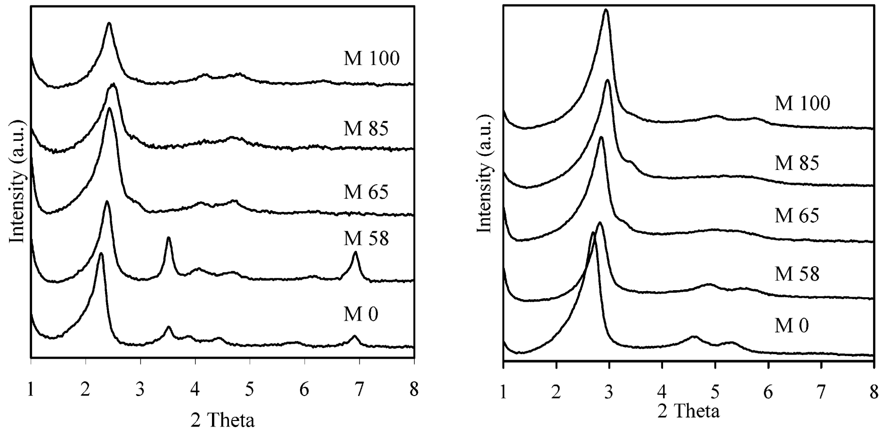

Figure 9. X-ray diffractograms of the different silica mesophases formed with increasing concentrations of methanol: (A) precursor materials; (B) calcined materials.

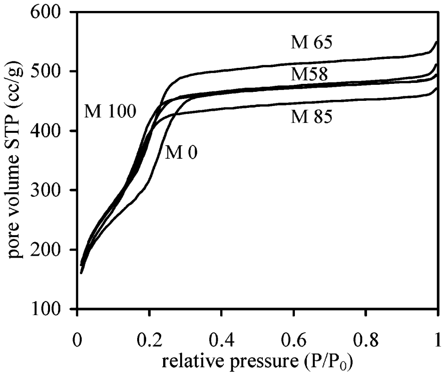

Figure 10. N_2 adsorption isotherms of the different silica mesophases formed with increasing concentations of methanol.

particle will also be responsible for the irregular morphology of the particles as observed with SEM.

With a doubling of the alcohol concentration compared to the MCM-48 phase, more alcohol will penetrate inside the micelles decreasing by the same occasion the surface curvature. This will inevitably lead to the formation of a lamellar phase. This is clear when comparing the X-ray diffractograms before and after calcination. After calcination part of the diffraction signal disappears. The remaining peak after calcination indicates that some ordering, other than a lamellar phase, must exist. TEM could not reveal a straightforward phase ordering suggesting that the structured arrangement must be very unstable under the applied electron beam. Important information in this respect is obtained from the isotherm of this phase. The low relative pressure data tend to show the same shape as the MCM-48 sample. This suggests the presence of some MCM-48-like unit cells. This strongly sustains the idea that ethanol could not decrease homogeneously the surface curvature to engage a logical phase transition from a cubic MCM-48 phase to a lamellar structure. Alcohol present inside the micelles will only disturb the formation and ordering of an identifiable phase, leaving MCM-48-like unit cells behind.

Upon further increasing the alcohol content, spherical particles are observed by SEM, as well as by TEM. The latter technique also reveals a remarkable phase regression phenomenon by showing pores organized in a hexagonal closed packing phase. This is confirmed by the bulk crystallographic analysis with XRD. It shows a hexagonal diffraction pattern with a (100), (110), and (200) diffraction signal. However, the TEM image seems to indicate that the ordering occurs only on a small scale. The FT pattern in the inset of Figure 6 shows very weak hexagonally arranged spots compared to the intense dots observed in the clear MCM-41 mesophase of Figure 4. This local hexagonal packing is a consequence of the radial arrangement of the pores.

A tentative explanation for this phase regression can be as follows. First, consider the changes on the level of micelle formation. At a high concentration, more and more alcohol molecules reside on the outer boundaries of the surfactant micelles, so the ratio of alcohol in the aqueous solution to that in the micelles is expected to increase. This means that the role of the alcohol is shifting from a cosurfactant to a cosolvent function. This cosolvent will have a diluting effect on the eventual micelles making them less packed, which automatically favors high surface curvatures. Second, the high concentration of alcohol in the solution will slow the hydrolysis reaction of TEOS to a large extent because of a preferential solvating into the alcohol phase. A restrained hydrolysis of TEOS decreases the number of charged silicate particles in the solution. Such less charge compensating solution enhances the repulsive forces between the adjacent headgroups of the surfactant molecules. Consequently, the effective headgroup surface area, a_0, of the surfactant molecules becomes larger, and the g value decreases in favor of the formation of a hexagonal phase or even at high surface curvature to some globular micelles. This preferential dissolution of TEOS into the alcohol will also help the mother solution to homogenize and thus to influence the type of silicate species formed during the hydrolysis process. Once the negatively charged hydrolysis products are formed, they will slowly replace the bromides as counterions of the cationic surfactants to electrostatically neutralize them, because bromide is known to be a strong binding anion.[19] Moreover, also the chosen reaction conditions of room temperature and the use of ammonia instead of sodium hydroxide as the base promote a slowing of the hydrolysis of the TEOS molecules.

The slow hydrolysis of TEOS forming a variety of silicate species in the solution, the disturbed mechanism of charge matching between the silicate species and the CTAB surfactant, and the potential delayed condensation of silicate–surfactant aggregates are all due to the massive presence of alcohol at the inorganic–organic interface. It all contributes to the complex mechanism, which provides the growth of the rather straight micelles on the surfaces of the center particles.

The growth will be fed by the addition of globular or straight silica-coated micelles.[12,20] The polymerization of the silicate walls will force those long flexible micelles to adopt a closed packing and thus a hexagonal ordering. When the micelle length is further increased, the high flexibility of long micelles could induce a loss of the order resulting in a more wormhole-like structure as shown near the outer limit region the particle (Figure 6).

The morphology of a growing particle (spherical or more irregular forms) depends on the balance between the rate of polymerization of the negatively charged silicate micelles and the rate of mesostructure formation.[21] In case of a slow polymerizing silicate seed at high alcohol concentrations, as in the Stöber silica synthesis,[22] the growth is driven by global surface tension forces to minimize its surface free energy by forming the shape of a sphere, as observed by SEM and TEM. In contrast, at lower alcohol concentrations, the polymerization will be relatively faster and the morphology will be controlled by the deposition of silicate-micellar species onto specific regions of the growing seed crystal resulting in nonuniform agglomerated blocks, as observed by SEM.

Although the Stöber synthesis can explain why a particle adopts a spherical shape, it does not give a clear explanation why the pores are arranged in a preferentially radial geometry.

In the logical order of the g-packing parameter, it could be that during the nucleus formation the micelles are ordered in a cubic symmetry. A further homogeneous micelle growth on the different planes of a cube will favor the radial arrangement of the micelles. This however needs more evidence by a detailed TEM study, which is under way.

Comparison Between the Different Alcohols. The relation between the mesophase and the added alcohol amount is different for propanol, ethanol, and methanol. The boundaries between adjacent phases are shifting to higher alcohol concentrations for the sequence propanol → ethanol → methanol. In other words, the amount of alcohol needed for obtaining a similar new phase is increasing with decreasing chain length of the alcohol. For example, 8 mol of propanol, 20 mol of ethanol, and 65 mol of methanol are required to obtain the MCM-48 phase. Because the alcohol's molar volume increases with increasing carbon chain lengths, it is evident that less alcohol is needed for the longer chained alcohols. Moreover, it has been proven that the amount of alcohol, which is located inside the micelles, increases exponentially with the increase of the alcohol's chain length.[23] This explains the observed differences in alcohol concentrations for the formation of new mesophases. Also the divergence in the obtained lamellar phases can be related to this phenomenon: for propanol, a pure lamellar phase is obtained in sample P14, the X-ray diffraction peaks of which fully disappear after calcination. In case of ethanol, a less obvious lamellar phase only gives rise to a broadening of XRD peaks, while for methanol no direct proof in XRD is found for the existence of a lamellar phase.

Another interesting observation is the occurrence of the phase regression point at 30, 58, and 100 mol for propanol, ethanol, and methanol, respectively. This indicates that not the concentration but the hydrophobic character of the alcohol has an influence on the phase regression point. This hydrophobic character has undoubtedly a certain effect on the hydrolysis rate of the TEOS and will therefore indirectly affect also the synthesis of the mesoporous phase.

Conclusions

Increasing amounts of alcohol, such as ethanol, propanol, and methanol, in the synthesis mixture of M41S materials results in a mesophase transition sequence: MCM-41→ MCM-48→ lamellar → radially arranged hexagonal closed packed mesophase (HCPM). When small amounts of alcohol are added, the alcohol molecules are located mainly inside the micelles acting as cosurfactants. Therefore, the g value increases and favors a phase transition from higher curved MCM-41 phase to a lower curved MCM-48 and lamellar phase. Further addition of alcohol leads to a situation in which the alcohol mainly acts as a cosolvent, decreasing the polarity of the solution. Spherical particles with hexagonal close packed pores arranged in a radial formation are formed. This is the result of a combination of (i) a decreased g-packing parameter value due to less tightly packed micelles and (ii) a very slow equilibrium toward the hydrolysis of TEOS due to solvating effects of the alcohol and its influence on the cooperative process of micelle formation, resulting in a slow growth of straight micelles on the surface of the center of the sperical particles. The polymerization of the silicate structure will force the micelles to adopt a close packed arrangement giving the hexagonal symmetry.

Acknowledgment. The authors thank K. Aerts for performing the SEM measurements. Financial support is also acknowledged by S. Liu for the exchange scholarship between the Chinese and Belgian governments. O. Collart is indebted to the IWT-Belgium for the Ph.D. grant. P. Cool and P. Van Der Voort acknowledge the FWO-Flanders Belgium for postdoctoral fellowships. The work was partially supported by the Belgian government through the IUAP V-1 network.

References and Notes

(1) Kresge, C. T.; Leonowicz, M. E.; Roth, W. J.; Vartuli, J. C.; Beck, J. S. *Nature* **1992**, *359*, 710.

(2) Corma, A. *Chem. Rev.* **1997**, *97*, 2373.

(3) Selvam, P.; Bhatia, S. K.; Sonwane, C. G. *Ind. Eng. Chem. Res.* **2001**, *40*, 3237.

(4) Ciesla, U.; Schuth, F. *Microporous Mesoporous Mater*. **1999**, *27,* 131.

(5) Cool, P.; Van Der Voort, P.; Vansant, E. F. In *Encyclopedia of surface and colloid science*; Hubbard, A., Ed.; Marcel Dekker Inc.: New York, 2002; p 5244.

(6) Linssen, T.; Cassiers, K.; Cool, P.; Vansant, E. F. *Adv. Colloid Interface Sci.* **2003**, *103*, 121.

(7) Trong, On D.; Desplantier-Giscard, D.; Danumah, C.; Kaliaguine, S. *Appl. Catal., A* **2001**, *222*, 299.

(8) Collart, O.; Van Der Voort, P.; Vansant, E. F.; Desplantier, D.; Galarneau, A.; Di Renzo F.; Fajula F. *J. Phys. Chem. B* **2001**, *105*, 12771.

(9) Alfredsson, V.; Anderson, M. W.; Ohsuna, T.; Terasaki, O.; Jacob, M.; Bojrup, M. *Chem. Mater.* **1997**, *9*, 2066.

(10) Huo, Q.; Margolese, D. I.; Stucky, G. D. *Chem. Mater.* **1996**, *8*, 1147.

(11) Landry, C. C.; Tolbert, S. H.; Gallis, K. W.; Monnier, A.; Stucky, G. D.; Norby, P.; Hanson, J. C. *Chem. Mater.* **2001**, *13*, 1601.

(12) Ågren, P.; Linden, M.; Rosenholm, J. B.; Schwarzenbacher, R.; Kriechbaum, M.; Amenitsch, H.; Laggner, P.; Blanchard, J.; Schüth, F. *J. Phys. Chem. B* **1999**, *103*, 5943.

(13) Grün, M.; Unger, K. K.; Matsumoto, A.; Tsutsumi, K. *Microporous Mesoporous Mater.* **1999**, *27,* 207.

(14) Stöber, W.; Fink, A.; Bohn, E. *J Colloid Interface Sci.* **1968**, *26*, 62.

(15) Pauwels, B.; Van Tendeloo, G.; Thoelen, C.; Van Rhijn, W.; Jacobs, P. A. *Adv. Mater.* **2001**, *13*, 1317.

(16) Kremer, S. P. B.; Kirschhock, C. E. A.; Aerts, A.; Villani, K.; Martens, J. A.; Lebedev, O. J.; Van Tendeloo, G. *Adv. Mater.*, in press.

(17) Gallis, K. W.; Landry, C. C. *Chem. Mater*. **1997**, *9* (10), 2035.

(18) Iler, R. K. *The Chemistry of Silica*; Wiley-Interscience publications: New York, 1979.

(19) Yang, H.; Vovk, G.; Coombs, N.; Sololov, I.; Ozin, G. A. *J. Mater. Chem*. **1998**, *8*, 743.

(20) Galarneau, A.; Di Renzo, F.; Fajula, F.; Mollo, L.; Fubini, B.; Ottaviani, M. F. *J. Colloid Interface Sci.* **1998**, *201*, 105.

(21) Chan, H. B. S.; Budd, P. M.; Naylor, T. V. *J. Mater. Chem.* **2001**, *11*, 951−957.

(22) Leite, C. A. P.; de Souza, E. F.; Galembeck, F. *J. Braz. Chem. Soc.* **2001**, *12* (4), 519.

(23) Eda, Y.; Takisawa, N.; Shirahama, K. *Langmuir* **1997**, *13*, 2432.